

Mathematical Modeling for Stress Distribution in Total Hip Arthroplasty

S. Srimongkol, S. Rattanamongkonkul, A. Pakapongpun, D. Poltem

Abstract—Stress distribution in total hip arthroplasty is the important tool to indicate the crack or failure of the total hip arthroplasty. Thus, this paper focuses on stress distribution in cemented hip arthroplasty which is affected by static and dynamic loads. Governing equations used in the simulation consists of stress equilibrium equations, the geometric equation and constitutive equations. Numerical results show that different loads lead to different stress distribution. Moreover, higher load increases stress in the top part of cemented hip arthroplasty. It is indicated that not only implant design affect total hip arthroplasty but also patient activity affect the life span of the total hip arthroplasty.

Keywords—Total hip arthroplasty, Total hip replacement, Stress distribution, Mathematical model, Dynamical loading, Finite element method

I. INTRODUCTION

The severity hip injury is usually treated by surgery known as total hip arthroplasty or total hip replacement. Although total hip arthroplasty is a high success rate treatment, the failure or loosening of total hip arthroplasty still occurs in 10-15 years after surgery [51], [34]. This causes problem to younger patients who live longer. If the joint wears out, a replacement implantation which causes higher risk than the first implantation may be performed. Congenital dislocation, hemorrhage, duration of the operation, intra-pelvic extrusion of cement are caused of revision arthroplasty [8].

To investigate the total hip replacement, the structure of bone is important using in the model. Bones contain blood vessels, nerve cells and living bone cells known as osteocytes. The outer hard part contains non-living material, calcium and phosphorous. The surface of the bone is covered with a thin membrane namely periosteum. The center of a long bone, such as a femur, is occupied by red bone marrow and yellow bone marrow. The red bone marrow is a soft tissue containing stem cells which produce blood cells, whereas the yellow bone marrow stores fat. The hard part of the bone can either be spongy or compact: the spongy or cancellous bone is light weight and is made up of connective tissues with large spaces between them; the compact or cortical bone is dense and forms

the outer layer of the bones. Compact bone is 5% to 30% porous, and cancellous bone is 30% to 90% porous [42]. The structure of long bone is shown in Fig. 1.

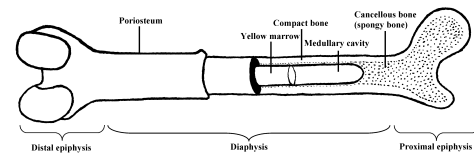


Fig. 1. Structure of long bone.

There are several research of mathematical model of bone remodeling process [36], [7]. The effects of parathyroid hormone, calcitonin, and vitamin D are investigated using a system of nonlinear differential equations. Both theoretical and numerical results show that the model is able to exhibit a periodic behavior observed in the clinical evidence.

Cemented and uncemented total hip arthroplasty are two major techniques using in the surgery. The use of uncemented femoral stem in primary total hip arthroplasty has developed slowly because of the lack of encouraging published long-term follow up data, the continued success of cemented hip arthroplasty, and the perceived excessive relative cost of the uncemented total hip arthroplasty [52]. Due to the fast recovery, the most surgeon use the cemented hip arthroplasty in the operation. Moreover, the intact cement-implant bond reduces the cement mantle stresses 35-60 % [16].

Aseptic loosening is a loosening of the total joint without involvement of bacteria. There are two theories for the cause of this including a mechanical theory and a biological theory [40]. In the mechanical theory, aseptic loosening is assumed to be a result of stress. Daily activities impose repeated cyclic stresses on the interlock between the total hip prosthesis and the bone, and the hip joints cannot adapt themselves to these stresses in the way that healthy joints can. Consequently, the bone cement then cracks and leads to aseptic loosening of the prosthesis.

The biological theory was developed after surgeons began to study the soft tissues around the loosening. These tissues produced enzymes and other substances which supported the dissolution of bone. It was also found that the soft tissues contained a lot of tiny wear particles with different origins, such as ceramic joint surfaces, metallic joint surfaces, and bone cement. These particles spread into the tissues around the artificial joint and provoked an inflammation reaction. The soft tissue created by this reaction had osteolytic properties

S. Srimongkol is with the Department of Mathematics, Faculty of Science, Burapha University, and Centre of Excellence in Mathematics, PERDO, CHE, THAILAND e-mail: sineenart@buu.ac.th.

S. Rattanamongkonkul is with the Department of Mathematics, Faculty of Science, Burapha University, and Centre of Excellence in Mathematics, PERDO, CHE, THAILAND e-mail: sahattay@buu.ac.th.

A. Pakapongpun is with the Department of Mathematics, Faculty of Science, Burapha University, and Centre of Excellence in Mathematics, PERDO, CHE, THAILAND e-mail: apisit.buu@gmail.com.

D. Poltem is with the Department of Mathematics, Faculty of Science, Burapha University, and Centre of Excellence in Mathematics, PERDO, CHE, THAILAND e-mail: duangkamolp@buu.ac.th.

which dissolved the bone. This bone dissolving process is called osteolysis.

When a total hip implant becomes loose, patients usually notice that pain increases around the joint, slight motion is found in the joint, and it is hard to put weight on the joint. The discomfort and pain usually develop slowly after an operation. However, in a minority of patients, the new artificial joint never functions well, and the pain and other discomfort increase steadily after the operation. When both components of the implant become loose, patients usually experience pain in the whole hip area and in the thigh. When only the femoral component becomes loose, patients usually experience pain mainly in the thigh. In addition to the increasing and lasting pain and stiffness in the hip, loosening of the implant is also typically accompanied by radiological changes.

In the beginning of hip surgery, the success rates were very low because the surgery was limited by trauma or infection. In 1847, anaesthesia and the antiseptic methods were introduced and success rates for surgery began to increase [17]. Major advances have been made in the years since 1847. However, in this thesis we will only discuss some of the important advances made since 1970. Riska (1970) [38] reviewed 470 cases of hip surgery to find factors affecting the primary mortality of patients with fractures of the femoral neck. The number of patients who die within 1 month of the injury or operation was 18.5 percent of the total cases. The death occurred from bronchopneumonia, hypostatic pneumonia, pulmonary embolism, cerebrovascular accident, and coronary thrombosis. Walker et al. (1971 [45]), Dandy (1972, [9]), Weightman et al. (1973, [47]), Weightman et al. (1973, [48]), Jan Modig et al. (1973-1974, [28]), and Dumbleton et al. (1974, [12]) have focused on the infection, prosthesis failure and wear. Some results indicate that increasing the molecular weight of polyethylene may improve the wear resistance.

The surgical management of osteoarthritis, aseptic necrosis and rheumatoid arthritis has been revolutionized by using acrylic cement to stabilize joint surface replacement. Early studies of acrylic bone cement were carried out by Urist (1975, [44]), Markolf et al. (1976, [26]), and Yettram et al. (1979, [53]). Yettram et al. (1979, [53]) used a two-dimensional finite element method to determine the normal and shear stress distributions on the prostheses-cement and cement-bone interfaces in the femoral component of a total hip replacement. Various combinations of stem, cement and bone stiffness were investigated. In particular the influences of stem taper, cement stiffness and prosthesis stiffness on the cement stresses were examined and compared. It was found that stresses increased as the stiffness of the stem decreased.

Yettram et al. (1980, [54]) used a two dimensional finite element method to determine the direct tensile stress distributions along the lateral edge of the stem of the femoral component of a total hip replacement. Various combinations of stem and cement stiffness were investigated. In particular, the influences of stem taper, cement stiffness and prosthesis stiffness were examined and compared. The most significant factor was found to be the modulus of elasticity of the stem material. The tensile stresses were found to decrease with decreasing modulus. Cement stiffness and stem shape appeared to have

less effect on the stem stress.

Patient's pain due to infection after hip replacement surgery is a significant clinical and diagnostic problem [50], [13], [18], [49], [5], [30], [19]. Jalovaara and Puranen (1989, [19]) investigated the air bacterial and particle counts which were present in a conventionally ventilated operating room. They suggested that using surgical textiles of non-woven material improved the purity of the operating room because, unlike cotton fabrics, they did not produce and disperse particles into the air.

The interlock between the cement and bone at the cement-bone interface is generated when the cement is injected in a doughy state and polymerizes in situ. Cement pressurization is required to ensure that the cement flows through the cancellous bone. It has been suggested that the failure of PMMA cement occurs as a consequence of cracking of the cement [10]. Many problems also occur in the laboratory such as errors from the calibration of the cement pressurization equipment and evaluation of cementation techniques. Errors in communication between the operating staff during the operation may also occur.

In order to understand the factors affecting the life span of an implant, a number of in vivo and in vitro experiments have been conducted [1], [4], [6]. McCaskie et al. (1997, [27]) tried to improve interlock between cement and bone around the femoral stem by using high pressure and by reducing the viscosity of cements. Funk and Litsky (1998, [14]) performed shear tests of the bone-cement interface in vitro using PMMA and polybutyl methacrylate (PBMA). Lennon and Prendergast (2002, [24]) investigated the residual stress due to shrinkage of PMMA bone cement after polymerization. This shrinkage is an important factor since it is capable of initiating cracks in the mantle of cemented hip replacements. They concluded that cracks were induced by residual stress around pores or other stress raisers.

Musculoskeletal loading and nerve palsy are main factors of failure or loosening of hip arthroplasty [23], [8]. Turner et al. [43] pointed out that the failure of implants is often associated with stress which is caused by load sharing between bone and implant. Complications of the hip replacement are often caused by the distribution of mechanical stresses over the implant-bone, bone-cement, or cement-implant interface [22]. Some clinical studies show that implant failure usually starts on the bone-cement interface and the implant-cement interface [25], [33].

The study of cancellous bone stresses surrounding the hip implant including the effect of elastic-plastic properties of cancellous bone is found that the poor quality of cancellous bone leads to failure of proximal femoral implant [41]. Probabilistic finite element analysis is used to study the effect of femur characteristics and implant design geometry of the uncemented hip arthroplasty [11]. Patterns of stress distribution in uncemented hip replacement is changed by using different loading [20]. The running biomechanical characteristics have an associated laterality movement [32]. To achieve normalization of the hip and pelvis kinematics and consequently normalize hip load, physical therapy in the early post-operative phase should focus on stretching of anterior and medial structures and

strengthening of hip flexors and abductors [23].

Numerical simulation of three dimensional total hip displacement has been used to study the effect of static loads with patient body weight 700, 1000, and 2000 N [2]. Base on finite element method, the result showed that higher weight provided higher displacement and von Mises stress affected the lateral femur.

Effect of heat transfer in the cemented hip arthroplasty is investigated [21]. The computational domain consists of three subregions which are implant, femoral canal, and femur bone. The mathematical model is governed by unsteady heat equation. Numerical results show that the initial temperature affects the total hip arthroplasty.

Several investigators [31], [56] have used the finite element method to study the effect of the residual stresses on the cement-bone and cement implant interfaces which are caused by temperature after the polymerization of bone cement. Cemented implants can show relative slop or micromotion at the cement-bone interface. These relative motions can increase with time and loading cycles, but remain small until progressive failure of the interface begins. The surface of the implant can be polished or matt. The stresses with polished surface implants are higher than with matt surface implants [24]. A more anatomically shaped prosthesis showed lower cement strains than a straight tapered prosthesis [34]. When a remodeling hip replacement is required, the femoral head must be resurfaced. In a resurfaced femoral head, strain in the proximal femoral head decreases when cement thickness increases [35]. In the patient who requires a hip and knee arthroplasty, there are hip-knee stems available. Hip-knee stem diameter is a major factor producing stress [46]. The prosthesis can be safe against fatigue under the static loading but fail under dynamic repetitive loading [39], [55].

The bone cement is subjected to high mechanical stress in the body. In vivo, the biomechanical situation is rather complex, involving different types of loading [29] such as bending, compression and shear, all of which must be tested. As the cemented implant is subjected to static loads and dynamic loads, the fatigue properties of the bone cement affect survival of the implant. In vivo loads at the hip joint are required to test and improve wear, strength, and stability of hip implants. Average patient load on the hip joint is 238 % of body weight during walking about 4 km/h [3]. Under the walking condition, the horizontal load components had a significant affect on the lubrication film of a metal on metal total hip implant [15]. This shows the importance of stress distribution using realistic loading and motion condition in the study of total hip arthroplasty. Therefore, the study of the effect of loads is crucial in the cemented total hip replacement. In this paper, the effect of static and dynamic loads on the implant, cement mantle and femur bone in total hip arthroplasty is investigated.

II. MATHEMATICAL MODELING

In the cemented total hip arthroplasty, the damaged hip joint is replaced by a hip prosthesis consisting of a metal or ceramic ball attached to a metal stem which is fitted into the femur.

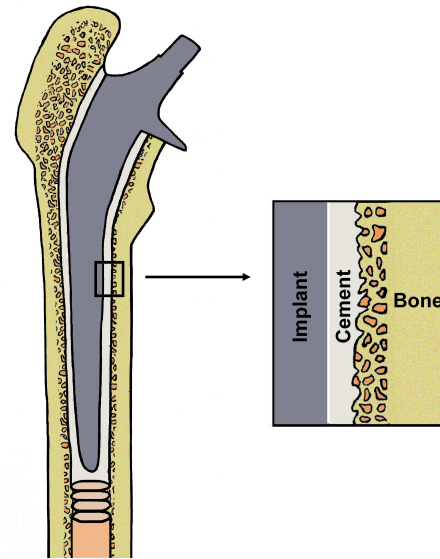


Fig. 2. Cemented hip replacement.

Bone cement is used to fix the prosthesis to the skeleton. The main components of cemented total hip arthroplasty which consists of implant, cement and bone is shown in Fig. 2.

As the performance and success of cemented total hip arthroplasty is related to the stress fields in the hip prosthesis-cement mantle-bone assembly, a mathematical model is constructed to analyze the stress field in the artificial hip component. The model is included stress due to the loading caused by patient activities. In the following, the mathematical model of the assembly is described, and then the field equations and boundary conditions governing the deformation and stress fields in the hip components are presented.

A. Governing Equations

From the principles of continuum mechanics, the field equations governing the arthroplasty and stress fields in the implant, cement mantle and bone include the stress equilibrium equations, the geometric equation and constitutive equations. These equations, in index notation, are as follows:

$$\rho \frac{\partial^2 u_i}{\partial t^2} - \sigma_{ij,j} = f_i \quad (i = 1, 2), \quad (1)$$

$$\varepsilon_{ij}(\mathbf{u}) = \frac{1}{2}(u_{i,j} + u_{j,i}), \quad (2)$$

$$\sigma_{ij} = (C_{ep})_{ij} \varepsilon_{ij}, \quad (3)$$

where σ and ε denote the stress tensor, and strain tensor respectively, \mathbf{u} is displacement, f_i represents body force, C_{ep} is the constitutive matrix.

To simulate the stress field corresponding to the patient activities, we impose two types of boundary conditions. On the base, displacement is restricted in the vertical direction. On the femoral head external load is imposed to simulate the force acting on the object corresponding to patient's activity. In this study, we consider two different cases: static and dynamic

TABLE I
FOURIER COEFFICIENTS USED IN THE COMPUTATION

i	1		2	
\bar{f}_i	37.28		128.3	
n	a_n	b_n	a_n	b_n
1	-22.09	14.07	-34.62	90.22
2	-22.62	44.62	13.06	22.45
3	23.46	18.61	-24.7	17.96
4	11.28	1.427	-1.159	-2.701

TABLE II
GOODNESS OF FIT OF FOURIER SERIES APPROXIMATION

Goodness of fit	f_1	f_2
Sum of squares due to error (SSE)	7.014	221
Coefficient of determination (R-square)	0.9978	0.9962
Degree-of-freedom adjusted coefficient of determination (Adjusted R-square)	0.9785	0.9616
Root mean squared error (RMSE)	2.648	14.87

loads. The static load is used for a patient with 50 kg body weight. The dynamic load is obtained from in vivo study [3]. Since, computational domain is two dimensions and the load in y-direction is very small, walking load in y-direction is then neglected. To use the dynamic load in the simulation, the fourier series approximation is applied to fit the graph of walking load. The result is shown in Figure 3.

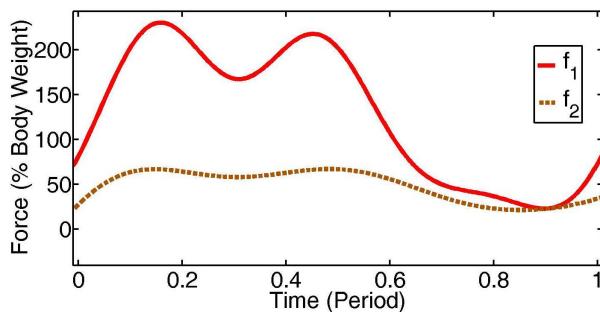


Fig. 3. Walking load: dash line and solid line represents f_1 and f_2 , respectively. X axis represents time period (1 period = 1.11 s) and Y axis represents force (% of body weight).

The walking load can be written in the form of the following Fourier series:

$$f_i(t) = \bar{f}_i + \sum_{n=1}^4 [a_n \cos n\omega t + b_n \sin n\omega t] \quad (4)$$

where \bar{f}_i is the mean loading, ω is 3.39, and the fourier coefficients (with 95% confidence bounds) are shown in the Table I.

The goodness of fit is shown in Table II. Sum of squares due to error measures the total deviation of the response values from the fit to the response values. Sum of squares due to error for f_1 and f_2 are 7.014 and 221, respectively. The value of f_1 is quite closed to 0 but the value of f_2 is much greater than 0 but still not too much in this case. It indicates that the model has a small random error component, and the fit will be useful. R-square is the square of the correlation between the response values and the predicted response values. R-square can take on any value between 0 and 1. R-square for f_1 and f_2 are 0.9978

and 0.9962, respectively. The values are closed to 1 therefore the great proportion of variance is accounted to the model. Degrees of freedom adjusted coefficient of determination uses the R-square and adjusts it based on the residual degrees of freedom. The adjusted R-square statistic is generally the best indicator of the fit quality when you compare two models that are nested. Since, adjusted R-square for f_1 and f_2 are 0.9875 and 0.9616, respectively and the values are closed to 1, it indicates that the fit is good. Finally, root mean squared error or standard error is an estimate of the standard deviation of the random component in the data. The values for f_1 and f_2 are 2.648 and 14.87, respectively which are closed to 0. It is indicated that the approximation is well fit. Thus, the fourier approximation of the graph is well fit.

B. Finite Element Formulation

To find the solution of the boundary value problem, the finite element method is used. The typical domain is denoted by Ω and standard weighted residual technique is applied [37]. Equations (1), (2), and (3) can be written in the following

$$\rho \frac{\partial^2 u}{\partial t} - \left(\frac{\partial \sigma_x}{\partial x} + \frac{\partial \sigma_{xy}}{\partial y} \right) = f_x \quad (5)$$

$$\rho \frac{\partial^2 v}{\partial t} - \left(\frac{\partial \sigma_{xy}}{\partial x} + \frac{\partial \sigma_y}{\partial y} \right) = f_y \quad (6)$$

where

$$\varepsilon_x = \frac{\partial u}{\partial x}, \varepsilon_y = \frac{\partial v}{\partial y} \text{ and } 2\varepsilon_{xy} = \frac{\partial u}{\partial y} + \frac{\partial v}{\partial x} \quad (7)$$

with

$$\begin{bmatrix} \sigma_x \\ \sigma_y \\ \sigma_{xy} \end{bmatrix} = \begin{bmatrix} d_{11} & d_{12} & 0 \\ d_{21} & d_{22} & 0 \\ 0 & 0 & d_{33} \end{bmatrix} \begin{bmatrix} \varepsilon_x \\ \varepsilon_y \\ 2\varepsilon_{xy} \end{bmatrix} \quad (8)$$

Equations (6) and (7) can be written in the term of the displacements u and v by substituting equation (7) into (8), and the result into (9) and (10):

$$-\frac{\partial}{\partial x} \left(d_{11} \frac{\partial u}{\partial x} + d_{12} \frac{\partial v}{\partial y} \right) - \frac{\partial}{\partial y} \left[d_{33} \left(\frac{\partial u}{\partial x} + \frac{\partial v}{\partial y} \right) \right] = f_x - \rho \frac{\partial^2 u}{\partial t^2} \quad (9)$$

$$-\frac{\partial}{\partial x} \left[d_{33} \left(\frac{\partial u}{\partial y} + \frac{\partial v}{\partial x} \right) \right] - \frac{\partial}{\partial x} \left(d_{12} \frac{\partial u}{\partial x} + d_{22} \frac{\partial v}{\partial y} \right) = f_y - \rho \frac{\partial^2 v}{\partial t^2} \quad (10)$$

To develop a variational statement corresponding to the BVP, we consider the following alternative problem.

Weak form of the governing differential equations.

Find u and $v \in H^1(\Omega)$ such that for all the weight functions w_1 and $w_2 \in H_0^1(\Omega)$, all the boundary conditions are satisfied, and we have

$$0 = \int_{\Omega} \left[\frac{\partial w_1}{\partial x} \left(d_{11} \frac{\partial u}{\partial x} + d_{12} \frac{\partial v}{\partial y} \right) + \frac{\partial w_1}{\partial y} d_{33} \left(\frac{\partial u}{\partial y} + \frac{\partial v}{\partial x} \right) - w_1 f_x + \rho w_1 \frac{\partial^2 u}{\partial t^2} \right] dx dy - \oint_{\Gamma} w_1 \left[\left(d_{11} \frac{\partial u}{\partial x} + d_{12} \frac{\partial v}{\partial y} \right) n_x + d_{33} \left(\frac{\partial u}{\partial y} + \frac{\partial v}{\partial x} \right) n_y \right] ds \quad (11)$$

$$0 = \int_{\Omega} \left[\frac{\partial w_2}{\partial x} d_{33} \left(\frac{\partial u}{\partial y} + \frac{\partial v}{\partial x} \right) + \frac{\partial w_2}{\partial y} \left(d_{12} \frac{\partial u}{\partial x} + d_{22} \frac{\partial v}{\partial y} \right) - w_2 f_y + \rho w_2 \frac{\partial^2 v}{\partial t^2} \right] dx dy - \oint_{\Gamma} w_2 \left[d_{33} \left(\frac{\partial u}{\partial y} + \frac{\partial v}{\partial x} \right) n_x + \left(d_{12} \frac{\partial u}{\partial x} + d_{22} \frac{\partial v}{\partial y} \right) n_y \right] ds \quad (12)$$

To find the numerical solution of the above problem, we pose the problem into the finite dimensional subspace. We choose N -dimensional subspace of $H_h \subset H^1(\Omega)$ for u and v and the corresponding test functions w_1 and w_2 . Let $\{\psi_j\}_{j=1}^N$ be the basis function of H_h , then we have

$$u(x, y, t) = \sum_{j=1}^N \psi_j(x, y) u_j(t) \quad (13)$$

$$v(x, y, t) = \sum_{j=1}^N \psi_j(x, y) v_j(t) \quad (14)$$

$$w_1(x, y, t) = \sum_{j=1}^N \psi_j(x, y) w_{1j}(t) \quad (15)$$

$$w_2(x, y, t) = \sum_{j=1}^N \psi_j(x, y) w_{2j}(t) \quad (16)$$

By substitute equations (13)-(16) into equations (11) - (12), and writing the resulting algebraic equations in the matrix form, we then obtain the system of ordinary differential equation

$$M\ddot{U} + A(U)U = F. \quad (17)$$

The equation (17) is a nonlinear system and can be solved by quasi-Newton method.

TABLE III

PARAMETERS USING IN THE SIMULATION OF THE DISPLACEMENT AND STRESS DISTRIBUTION IN IMPLANT, CEMENT MANTLE (PMMA), AND FEMUR BONE.

Parameters	Implant	PMMA	Femur	Units
Density (ρ)	4420	1100	1420	kg/m^3
Young's modulus (E)	21.0	0.228	1.5	$\times 10^{10} Pa$
Poisson's ratio (ν)	0.3	0.3	0.3	-

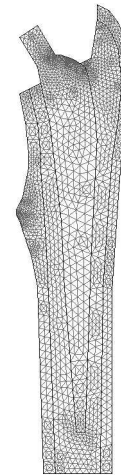


Fig. 4. Mesh of the implant-cement geometry consists of 4,132 triangular elements and 17,006 degrees of freedom.

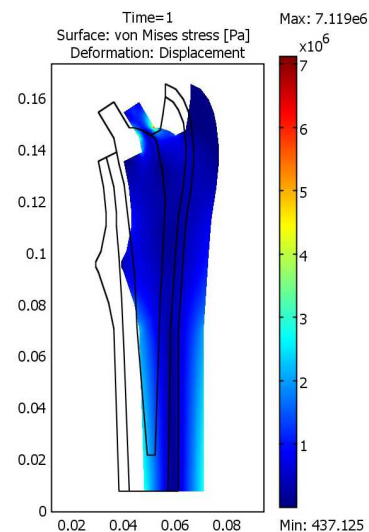


Fig. 5. Surface plot of von Mises stress for static load.

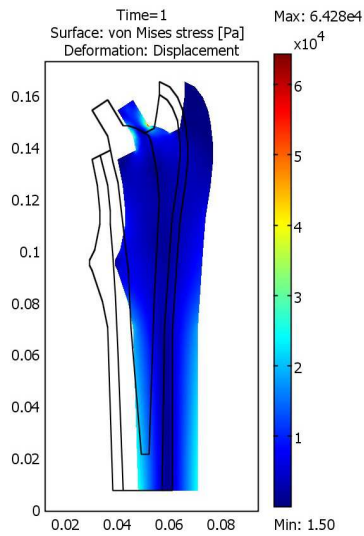


Fig. 6. Surface plot of von Mises stress for dynamic load.

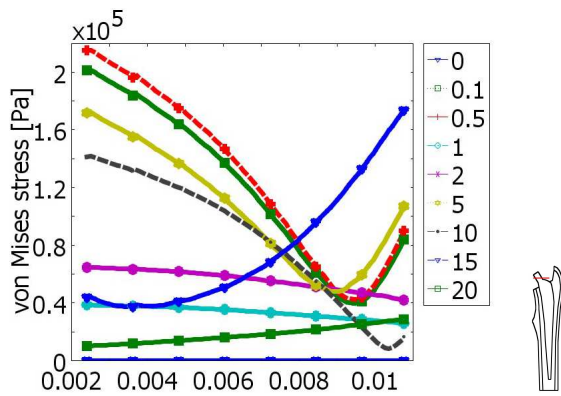


Fig. 7. Cross section of von Mises stress at different times.

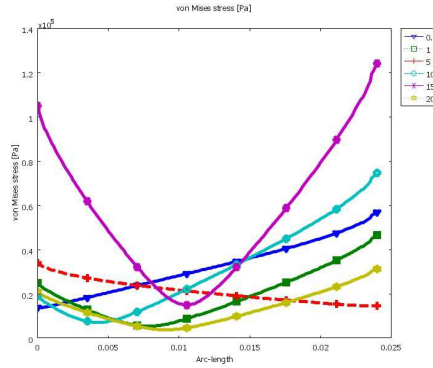


Fig. 8. Cross section of von Mises stress at different times.

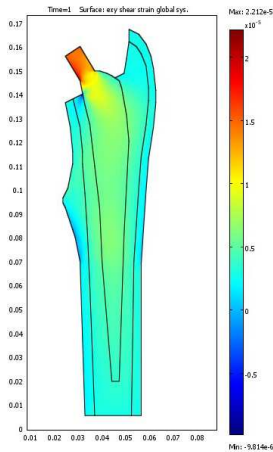


Fig. 9. Surface plot of shear strain at time 1 s for static load of (a) static load, and (b) dynamic load.

III. NUMERICAL RESULTS

Computational mesh generated by commercial package, COMSOL Multiphysics, consists of 4,132 triangular elements and 17,006 degrees of freedom is presented in Fig. 4. The parameters using in the simulation is summarized in Table III. The finite element method is used to find the numerical solution. The numerical result of von Mises stresses for the steady load is shown in Fig. 5. The high concentration of stresses occurs at the neck of the implant. The maximum and minimum von Mises stresses are 8.782379×10^6 and 3.940597×10^2 Pa, respectively. For dynamic load, the numerical result of von Mises stresses is shown in Fig. 6. The maximum and minimum values are 7.297044×10^4 and 1.349929 Pa, respectively.

The stress distribution for dynamic load at different times are different as shown in Fig. 7. The von Mises stresses of dynamic load are less than that for static load. Von Mises stress near the bone (right hand side of the total hip arthroplasty in the small figure of Fig. 8) is dropped at time 0.5, 5, 10 and 20 s. Figure 8 shows the von Mises stress at the lower part of the stem at different times. At time 15 s, von Mises is the parabolic shape, the stress at high at the outer part of the

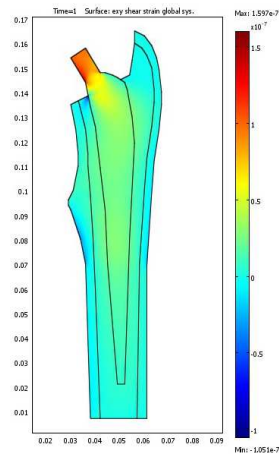


Fig. 10. Surface plot of shear strain at time 1 s for dynamic load.

bone. The effect of shear strain of shear strain for static and dynamic loads is shown in Fig. 9 and 10, respectively.

IV. CONCLUSION

The numerical results show that the von Mises stresses for dynamic load are less than that for static load. Since the dynamic load here is calculated from patient walking, when time changes the load applied to the hip also changes. This causes the load which applied to the hip is reduced. For the total shear strain, the numerical results show that the displacement for dynamic load is less than static load. However, the patient activity affects to the displacement. When patient have a lot of activities, the result should be the loosening of the total hip arthroplasty. Moreover, the high patient load will cause the loosening faster. Therefore, the patients with total hip arthroplasty have to take care for daily activity. The more activity results the fast loosening. Patients should reduce the load applied to the hip to increase the life span of the total hip arthroplasty. To predict the life span of the total hip arthroplasty, the more realistic modeling is necessary. Further work, it should be investigated the realistic three dimensional modeling of the system of the total hip arthroplasty.

ACKNOWLEDGMENT

This research is supported by faculty of science, Burapha university, Thailand. The authors are grateful to Prof. Benchawan Wiwatanapataphee for her helpful suggestions and comments on this paper. The authors would also like to thank the referee for valuable comments on an earlier version of this paper.

REFERENCES

- [1] P H Adegbile, B Russery, L Taylor, and J Tong, *Failure of an uncemented acetabular prosthesis a case study.*, *Engineering Failure Analysis* **13** (2006), no. 1, 163–169.
- [2] Somkid Amornsamankul, Kamonchat Kaorapong, and Benchawan Wiwatanapataphee, *Three-dimensional simulation of femur bone and implant in femoral canal using finite element method*, *International Journal of Mathematics and Computers in Simulation* **4** (2010), no. 4, 171–178.
- [3] G. Bergmann, G. Deuretzbacherb, M. Hellerc, F. Graichena, A. Rohlmanna, J. Straussb, and G. N. Dudac, *Hip contact forces and gait patterns from routine activities*, *Journal of Biomechanics* **37** (2001), no. 7, 859–871.
- [4] S L Bevill, G R Bevill, J R Penmetsa, A J Petrella, and P J Rullkoetter, *Finite element simulation of early creep and wear in total hip arthroplasty*, *J Biomech* **38** (2005), no. 12, 2365–74.
- [5] Gudmund Blomgren, Anna Hambræus, and Anna-Stina Malmborg, *Hygienic and clinical study of elective and acute hip operations*, *Journal of Hospital Infection* **3** (1982), no. 2, 111–121.
- [6] M Bohner, B Gasser, G Baroud, and P Heini, *Theoretical and experimental model to describe the injection of a polymethylmethacrylate cement into a porous structure*, *Biomaterials* **24** (2003), 2721–30.
- [7] Inthira Chaiya, Chontita Rattanakul, Sahattaya Rattanamongkonkul, Wannapa Kunpasuruang, and Sittipong Ruktamatukul, *Effects of parathyroid hormone and calcitonin on bone formation and resorption: mathematical modeling approach*, *International Journal of Mathematics and Computers in Simulation* **5** (2011), no. 6, 510–519.
- [8] Jacques E. Chelly, Anna A. Uskova, and Anton Plakseychuk, *The role of surgery in postoperative nerve injuries following total hip replacement*, *Journal of Clinical Anesthesia* **22** (2010), no. 4, 285 – 293.
- [9] D.J. Dandy, *Fat embolism following prosthetic replacement of the femoral head*, *Injury* **3** (1972), no. 2, 85–88.
- [10] F R Dimario, *The science of bone cement: a historical review*, *Orthopedics* **25** (2002), no. 12, 1399–407.
- [11] C. Dopico-González, A. M. New, and M. Browne, *Probabilistic finite element analysis of the uncemented hip replacement—effect of femur characteristics and implant design geometry*, *J. Biomech.* **43** (2010), 512–520.
- [12] J H Dumbleton, C Shen, and E H Miller, *A study of the wear of some materials in connection with total hip replacement*, *Wear* **29** (1974), no. 2, 163–171.
- [13] Helen Enright, Robert Haake, and Daniel Weisdorf, *Avascular necrosis of bone: A common serious complication of allogeneic bone marrow transplantation*, *The American Journal of Medicine* **89** (1990), no. 6, 733–738.
- [14] Michael J Funk and Alan S Litsky, *Effect of cement modulus on the shear properties of the bone-cement interface*, *Biomaterials* **19** (1998), 1561–7.
- [15] L. Gao, F. Wang, P. Yang, and Z. Jin, *Effect of 3d physiological loading and motion on elasto-hydrodynamic lubrication of metal-on-metal total hip replacements*, *Med. Eng. Phys.* **31** (2009), 720–729.
- [16] P. J. Gard, R. Oorio, and W. L. Healy, *Hip replacement: choosing and implant*, *Oper. Techn. Orthopaed.* **10** (2000), no. 2, 94–101.
- [17] Brian Neil Le Gros, *Three-dimensional, non-linear finite element analysis, and elastic modulus optimization of a geometry for a non-metallic femoral stem*, Master's thesis, Queen's University, Kingston, Ontario, Canada, October 2001.
- [18] C. Hill, F. Mazas, R. Flamant, and J. Evrard, *Prophylactic cefazolin versus placebo in total hip replacement report of a multicentre double-blind randomised trial*, *The Lancet* **317** (1981), no. 8224, 795–797.
- [19] P. Jalovaara and J. Puranen, *Air bacterial and particle counts in total hip replacement operations using non-woven and cotton gowns and drapes*, *Journal of Hospital Infection* **14** (1989), no. 4, 333–338.
- [20] I. Jonkers, N. Sauwen, G. Lenaerts, M. Mulier, G. Van der Perre, and S. Jaecques, *Relation between subject-specific hip joint loading, stress distribution in the proximal femur and bone mineral density changes after total hip replacement*, *J. Biomech.* **41** (2008), 3405–3413.
- [21] Kamonchat Kaorapong, Somkid Amornsamankul, I-Ming Tang, and Benchawan Wiwatanapataphee, *Heat transfer in cemented hip replacement process*, *International Journal of Mechanics* **5** (2011), no. 3, 202–209.
- [22] H. Katozian and D. T. Davy, *Effects of loading conditions and objective function on the three-dimensional shape optimization of femoral components of hip endoprostheses*, *Medical Engineering & Physics* **22** (2000), 243–251.
- [23] G. Lenaerts, M. Mulier, A. Spaepen, G. Van der Perre, and I. Jonkers, *Aberrant pelvis and hip kinematics impair hip loading before and after total hip replacement*, *Gait & Posture* **30** (2009), 296–302.
- [24] A B Lennon and P J Prendergast, *Residual stress due to curing can initiate damage in porous bone cement: experimental and theoretical evidence*, *J Biomech* **35** (2002), no. 3, 311–21.
- [25] K A Mann, R MocarSKI, L A Damron, M J Allen, and D C Ayers, *Mixed-mode failure response of the cement-bone interface*, *J Orthop Res* **19** (2001), 1153–61.
- [26] K. L. Markolf and H. C. Amstutz, *A comparative experimental study of stresses in femoral total hip replacement components: The effects of prostheses orientation and acrylic fixation*, *Journal of Biomechanics* **9** (1976), no. 2, 73–74.
- [27] A W McCaskie, M R Barnes, E Lin, W M Harper, and P J Gregg, *Cement pressurisation during hip replacement*, *Journal of Bone and Joint Surgery* **79** (1997), no. 3, 379–84.
- [28] Jan Modig, Sven Olerud, Per Malmberg, and Christer Busch, *Medullary fat embolization during total hip replacement surgery: a preliminary report*, *Injury* **5** (1973-1974), no. 2, 161–164.
- [29] M. Hilal Muftah and S. Mohamed Haris, *A strain gauge based system for measuring dynamic loading on a rotating shaft*, *International Journal of Mechanics* **5** (2011), no. 1, 19–26.
- [30] Carl W. Norden, *Prevention of bone and joint infections*, *The American Journal of Medicine* **78** (1985), no. 6, 229–232, Supplement 2.
- [31] N Nuno and G Avanzolini, *Technical note: Residual stresses at the stem-cement interface of an idealized cemented hip stem*, *J Biomech* **35** (2002), 849–52.
- [32] Corina Pantea, Adrian Ivan, Stelian Pantea, , and Mihaela Faur, *Study concerning the incidence of knee sprain and the biomechanical analysis during running at sportsmen who suffered from knee sprain*, *International Journal of Biology and Biomedical Engineering* **5** (2011), no. 2, 75–82.
- [33] M A Perez, J M Garcia, and M Doblare, *Analysis of the debonding of the stem-cement interface in intramedullary fixation using a non-*

- linear fracture mechanics approach*, Engineering Fracture Mechanics **72** (2005), 1125–47.
- [34] B Peter, N Ramaniraka, L R Pakotomanana, P Y Zambelli, and D P Pioletti, *Peri-implant bone remodeling after total hip replacement combined with systemic alendronate treatment: a finite element analysis*, Comput Meth Biomech Biomed Eng **7** (2004), no. 2, 73–8.
- [35] I.A.J. Radcliffe and M. Taylor, *Investigation into the affect of cementing techniques on load transfer in the resurfaced femoral head: A multi-femur finite element analysis*, Clin Biomech **22** (2007), no. 4, 422–30, doi:10.1016/j.clinbiomech.2006.12.001.
- [36] Sahattaya Rattanamongkonkul, Wannapa Kunpasuruang, Sittipong Ruktamatakul, and Chontita Rattanakul, *A mathematical model of bone remodeling process: effect of vitamin d*, International Journal of Mathematics and Computers in Simulation **5** (2011), no. 5, 489–498.
- [37] J. N. Reddy, *An introduction to the finite element method*, 2nd ed., McGraw-Hill series in mechanical engineering, McGraw-Hill, Inc., Singapore, 1993.
- [38] E B Riska, *Factors influencing the primary mortality in the treatment of hip fractures*, Injury **2** (1970), no. 2, 107–115.
- [39] A Z Senalp, O Kayabasi, and H Kurtaran, *Static, dynamic and fatigue behavior of newly designed stem shapes for hip prosthesis using finite element analysis*, Mater Design **28** (2007), no. 5, 1577–83.
- [40] Valdemar SURIN, http://www.totaljoints.info/th_loose_details.htm accessed on 23rd january 2007.
- [41] M. Taylor, K. E. Tanner, M. A. R. Freeman, and A. L. Yettram, *Cancellous bone stresses surrounding the femoral component of a hip prosthesis: and elastic-plastic finite element analysis*, Med. Eng. Phys. **17** (1995), no. 7, 544–550.
- [42] Tpta, <http://www.tpta.org/osteo/definition.htm>, accessed on 27th November 2006.
- [43] A W L Turner, R M Gillies, R Sekel, P Morris, W Bruce, and W R Walsh, *Computational bone remodelling simulations and comparisons with dexa results*, Journal of Orthopaedic Research **23** (2005), 705–12.
- [44] Marshall R. Urist, *Acrylic cement stabilized joint replacements*, Current Problems in Surgery **12** (1975), no. 11, 1–54.
- [45] P. S. Walker and B. L. Gold, *The tribology (friction, lubrication and wear) of all-metal artificial hip joints*, Wear **17** (1971), no. 4, 285–299.
- [46] P S Walker, W W Yoon, S R Cannon, G Bentley G, and S K Muirhead-Allwood, *Design and application of combined hip-knee intramedullary joint replacements*, J Arthroplasty **14** (1999), no. 8, 945–51.
- [47] B Weightman and I Paul, *An analytical model for wear applied to the design of total hip prostheses*, Wear **24** (1973), no. 2, 229–234.
- [48] Barry O. Weightman, Igor L. Paul, Robert M. Rose, Sheldon R. Simon, and Eric L. Radin, *A comparative study of total hip replacement prostheses*, Journal of Biomechanics **6** (1973), no. 3, 299–306.
- [49] W. Whyte, R. Hodgson, and J. Tinkler, *The importance of airborne bacterial contamination of wounds*, Journal of Hospital Infection **3** (1982), no. 2, 123–135.
- [50] Frank Williams, Iain W. McCall, William M. Park, Brian T. O'Connor, and Valerie Morris, *Gallium-67 scanning in the painful total hip replacement*, Clinical Radiology **32** (1981), no. 4, 431–439.
- [51] S R Wilson, *Hierarchical modelling of orthopaedic hip replacement damage accumulation and reliability*, Journal of the Royal Statistical Society Series C - Applied Statistics: Part 2 **425** (2005), 425–41.
- [52] Piers Yates, Shelley Serjeant, Graham Rushforth, and Robert Middleton, *The relative cost of cemented and uncemented total hip arthroplasties*, The Journal of Arthroplasty **21** (2006), no. 1, 102–105.
- [53] A. L. Yettram and K. W. J. Wright, *Biomechanics of the femoral component of total hip prostheses with particular reference to the stress in the bone-cement*, Journal of Biomedical Engineering **1** (1979), no. 4, 281–285.
- [54] A. L. Yettram and K.W.J. Wright, *Dependence of stem stress in total hip replacement on prosthesis and cement stiffness*, Journal of Biomedical Engineering **2** (1980), no. 1, 54–59.
- [55] N P Zant, C K Y Wong, and J Tong, *Fatigue failure in the cement mantle of a simplified acetabular replacement model*, Int J Fatigue **29** (2007), no. 7, 1245–1252.
- [56] Mehmet Zor, Mumin Kucuk, and Sami Aksoy, *Residual stress effects on fracture energies of cement-bone and cement-implant interfaces*, Biomaterials **23** (2002), 1595–601.